

Magnetic-field-dependent interplay between incoherent and Fermi liquid transport mechanisms in low-dimensional τ -phase organic conductors

K. Storr, L. Balicas, J. S. Brooks, and D. Graf

National High Magnetic Field Laboratory, Florida State University, Tallahassee, Florida 32306

G. C. Papavassiliou

Theoretical and Physical Chemistry Institute, National Hellenic Research Foundation, Athens, Greece 116/35

(Received 27 November 2000; revised manuscript received 22 February 2001; published 2 July 2001)

We present an electrical transport study of the two-dimensional (2D) organic conductor τ -[P-(S,S)-DMEDT-TTF]₂(AuBr₂) (AuBr₂)_y (where $y \sim 0.75$) at low temperatures and high magnetic fields. The interplane resistivity ρ_{zz} increases with decreasing temperature, with the exception of a slight anomaly at 12 K. Under a magnetic field B , both ρ_{zz} and the in-plane resistivity plane ρ_{xx} show a pronounced negative and hysteretic magnetoresistance. In spite of a negative residual resistivity ratio in zero field, Shubnikov-de Haas (SdH) oscillations are observed in some (high quality) samples above 15 T. Furthermore, contrary to the single closed orbit Fermi surface (FS) predicted from band structure calculations (where a single star-shaped FS sheet with an area of $\sim 12.5\%$ of A_{FBZ} is expected), two fundamental frequencies F_l and F_h are detected in the SdH signal. These orbits correspond to 2.4 and 6.8% of the area of the first Brillouin zone (A_{FBZ}), with effective masses $\mu_l = 4.4 \pm 0.5$ and $\mu_h = 7.5 \pm 0.1$, respectively. The angular dependence, in tilted magnetic fields, of F_l and F_h , reveals a 2D character of the FS, but no evidence for warping along the k_z direction (e.g., the absence of a beating effect in the SdH signal) is observed. Angular dependent magnetoresistance (AMRO) further suggests a FS which is strictly 2D where the interplane hopping t_c is virtually absent or incoherent. The Hall constant R_{xy} is field independent, and the Hall mobility μ_H increases by a factor of ~ 3 under moderate magnetic fields. Hence the field does not alter the carrier concentration, even in the presence of a large negative magnetoresistance, but only increases the lifetime τ_s . Our observations suggest a unique physical situation where a stable 2D Fermi liquid state in the molecular layers, are incoherently coupled along the least conducting direction. The magnetic field not only reduces the inelastic scattering between the 2D metallic layers, as seen in the large negative magnetoresistance and SdH effect, but it also reveals the incoherent nature of the interplane transport in the AMRO spectrum. Finally, the observed Fermi surface is at odds with band structure calculations. The observation of small pockets may suggest FS reconstruction. However, the very flat bands in the electronic structure, combined with the variable charge transfer, may be the origin of these effects. The apparent ferromagnetic character of the hysteresis in the magnetoresistance, remains an unsolved problem.

DOI: 10.1103/PhysRevB.64.045107

PACS number(s): 72.15.Gd, 72.15.Eb, 72.80.Le

I. INTRODUCTION

In the last two decades, the field of anisotropic low-dimensional organic conductors has become synonymous with the observation of unusual and exotic electronic properties. Examples range from the possibility of unconventional, anisotropic superconductivity,^{1,2} to the observation of a variety of other ground states such as charge-density waves (CDW's),³ spin-density waves (SDW's),⁴ field-induced spin-density waves (FISDW's) (associated with the observation of quantum Hall effect,⁵) and the spin-Peierls (SP) state.⁶ A considerable amount of effort has also been devoted to fermiology⁷ and the properties of the metallic states of these compounds. Non-Fermi-liquid-like behavior has been reported in photoemission spectra⁸ and there are indications of spin-charge separation⁹ in some materials. In addition, unconventional electrical transport properties in the presence of magnet-field induced incoherent hopping has been proposed.^{10,11}

More recently, new degrees of freedom are being added to these already physically rich systems by incorporating mag-

netic anions into the structure of organic compounds. Here, due to the physical separation of the molecular orbital (cation) layers, and the inorganic anion layers, there is a corresponding separation of the localized magnetic anion moments (for example, the d electrons) and the itinerant low-dimensional organic molecular electrons gas (π electrons). Typical examples are the series λ -(BETS)₂Fe_xGa_{1-x}Cl₄ compounds¹² and TPP[Fe(Pc)(CN)₂]₂.¹³ In the BETS series, the progressive substitution of Ga with Fe suppresses the superconducting state and stabilizes an insulating antiferromagnetic (AF) state.¹² While in TPP[Fe(Pc)(CN)₂]₂, the ground state is also insulating and presents an anisotropic magnetic susceptibility.

One of the main characteristics of magnetic organic systems as mentioned above is the observation of a pronounced or giant negative magnetoresistance under field. This effect has been explained in terms of field alignment of the local magnetic moments. On one hand, it is expected to destroy an eventual AF ground state, i.e., to close related gaps at the Fermi level (spin-flop transition),¹⁴ and on the other, to decrease the spin scattering of itinerant electrons by these local

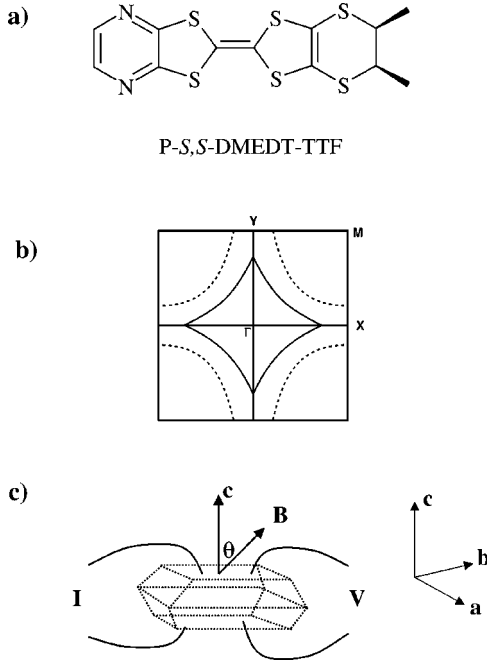


FIG. 1. (a) A sketch of the P-(*S,S*)-DMEDT-TTF molecule. (b) Calculated Fermi surface of τ -[P-(*S,S*)-DMEDT-TTF] $_2$ (AuBr $_2$) $_1$ (AuBr $_2$) $_y$ and for $y \sim 0.75$ (solid line). The dashed line represents the calculated Fermi surface for $y = 0$. (c) Configuration of contacts in relation to sample morphology for interplane electrical transport measurements.

moments. In any case, the necessary ingredients for explaining the magnetic-field induced enhancement of the conductivity in these compounds, seems to be the presence of localized magnetic moments, their interaction with itinerant electrons, and the effects of the magnetic field on this coupled system.

Nevertheless, there are other families of organic conductors, the compounds of the τ crystallographic phase,¹⁵ whose magnetoresistivity presents remarkable similarities to what is observed, for example, in λ -(BETS) $_2$ FeCl $_4$ and TPP[Fe(Pc)(CN) $_2$] $_2$, although their structure is *not* composed by any magnetic element, see Fig. 1(a). Here we report on the electrical transport properties of the τ -[P-(*S,S*)-DMEDT-TTF] $_2$ (AuBr $_2$) $_1$ (AuBr $_2$) $_y$ compound [where $y \sim 0.75$ and P-(*S,S*)-DMEDT-TTF stands for pyrazino-(*S,S*)-dimethyl-ethylenedithio-tetrathiafulvane], at high magnetic fields B and low temperatures T . In this compound, an in-plane as well as interplane magnetoresistivity is found to decrease by a factor $\geq 65\%$ when a field $B \leq 10$ T is applied. A significant hysteresis is also observed,¹⁶ which points towards the formation of field induced domains and has been interpreted as an indication of the magnetic nature of these compounds.¹⁷ However, magnetic susceptibility measurements revealed an almost temperature independent paramagnetic term. This term is comparable to those measured in other 2D nonmagnetic organic systems which are characterized by strong electronic correlations.¹⁸

The crystallographic structure of τ -[P-(*S,S*)-DMEDT-TTF] $_2$ (AuBr $_2$) $_1$ (AuBr $_2$) $_y$ is tetragonal with unit

cell dimensions $\mathbf{a} = \mathbf{b} = 7.3546$ Å and $\mathbf{c} = 67.977$ Å.¹⁸ Inorganic anion layers alternate with mixed organic-inorganic layers, which has both ordered and disordered AuBr $_2$ anions, along with a disordered ethylene group.¹⁸ The ratio of donor molecules to acceptor anions is $2:(1+y)$, where y has been estimated to be ~ 0.75 . The value of y determines the area of the Fermi surface, which decreases with increasing y .¹⁹ Figure 1(b) shows the calculated Fermi surface of τ -[P-(*S,S*)-DMEDT-TTF] $_2$ (AuBr $_2$) $_1$ (AuBr $_2$) $_y$, $y \sim 0.75$, which was calculated using the extended Hückel tight binding method.²⁰ The star shaped Fermi surface, results from the fourfold symmetry of the molecules packing. While the \mathbf{a} - \mathbf{b} plane is metallic (conducting) the interplane electrical transport displays an unusual nonmetallic behavior over the whole temperature range. This behavior contrasts with what is observed in most quasi-two-dimensional (Q2D) organic compounds, where a T^2 behavior at low T , is followed by a nonmetallic behavior at higher temperatures. A smooth crossover from coherent Fermi-liquid excitations at low temperatures, to incoherent excitations at high temperatures, has been suggested to occur in these compounds.²¹

In this paper, we report the observation of Shubnikov de Haas (SdH) oscillations in a τ phase organic conductor; the τ -[P-(*S,S*)-DMEDT-TTF] $_2$ (AuBr $_2$) $_1$ (AuBr $_2$) $_y$ compound. Two fundamental frequencies F_l and F_h were detected in the fast Fourier transform of the SdH signal, corresponding, respectively, to 2.4 and 6.8 % of the area of the first Brillouin zone (A_{FBZ}), which is at odds with band structure calculations. Relatively large effective masses (i.e., for nonsuperconducting organic conductors⁷) $\mu_l = 4.4 \pm 0.5$ and $\mu_h = 7.5 \pm 0.1$ were obtained for F_l and F_h , respectively. The angular dependence of F_l and F_h reveals the 2D character of the FS, and the absence of frequency beatings indicates that the FS has no detectable warping along the k_z direction. The angle dependent magnetoresistance (AMRO) further suggests a strictly 2D FS, where the interplane hopping t_c is virtually absent, or is incoherent. We find the Hall constant R_{xy} to be field independent, and the Hall mobility μ_H to increase by a factor of ~ 3 , under moderate magnetic fields. This indicates that B does not introduce additional carriers into the system, instead, it decreases the carriers scattering rate τ_s^{-1} . As neither the interplane nor the in-plane resistivity displays a T^2 dependence at zero field, we conclude, that the magnetic field induces a crossover from a ‘‘non-Fermi-liquid-like’’ behavior at moderate fields, towards a Fermi-liquid-type behavior at higher fields, whose signature is the observation of quantum oscillations, i.e., the Shubnikov–de Haas (SdH) effect.

II. EXPERIMENTAL RESULTS

Several different single crystals of τ -[P-(*S,S*)-DMEDT-TTF] $_2$ (AuBr $_2$) $_1$ (AuBr $_2$) $_y$ ($y \sim 0.75$), synthesized by electrochemical methods,²² were used in the present investigation. Gold wires of 12.5 μm were attached with graphite paint in a conventional four-terminal configuration for interlayer electrical transport measurements, see Fig. 1(c); while a six-terminal configuration was used for the Hall effect measurements. Standard low frequency (~ 20 Hz) ac

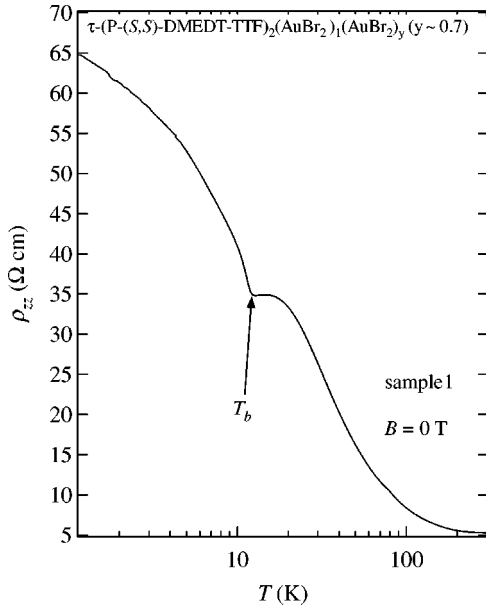


FIG. 2. Temperature dependence of the interplane resistivity ρ_{zz} of τ -[P-(S,S)-DMEDT-TTF] $_2$ (AuBr $_2$) $_1$ (AuBr $_2$) $_y$ ($y \sim 0.75$) at zero magnetic field. The change in slope observed at T_b is a characteristic anomaly in this material (see text).

lock-in techniques, with currents of order of 10 μ A were employed in the measurements. Samples were mounted in a variety of fixed as well as rotating sample holder probes, immersed in both 3 He cryostats and dilution refrigerators. Magnetic fields were provided by the resistive magnets available at the National High Magnetic Field Laboratory's dc field facility in Tallahassee Florida.

Figure 2 shows the typical temperature dependence at zero magnetic field of the interplane resistivity ρ_{zz} , of a τ -[P-(S,S)-DMEDT-TTF] $_2$ (AuBr $_2$) $_1$ (AuBr $_2$) $_y$ ($y \sim 0.75$) single crystal, sample No. 1. Although the in-plane resistivity displays a metallic behavior,²³ the interplane transport, as seen in the figure, is clearly nonmetallic and shows an abrupt change in slope at $T_b \approx 12$ K. At this temperature, a metal-insulator transition has been suggested to occur, although specific heat measurements did not provide any evidence for a phase transition¹⁸ at T_b . Below T_b , the *in-plane* resistivity, in contrast to the interplane resistivity, seems to follow a logarithmic dependence on temperature.²³ This dependence was interpreted as an indication of either weak localization^{18,23} or Kondo effect arising possibly from exchange interaction between localized magnetic moments and itinerant conduction electrons.²³ In any case, and as clearly seen, the interplane resistivity ρ_{zz} does not display the typical T^2 dependence seen at low T in other Q2D organic compounds, which is the signature of coherent electrical transport.²⁴

Figure 3 shows the temperature dependence of ρ_{zz} for $\theta \approx 0^\circ$ (θ is the angle between B and the c axis) and for several values of magnetic field B , as indicated in the figure. Several significant features are observed.

(i) Between T_a and 6 K, for increasing magnetic field ($B > 5$ T), ρ_{zz} exhibits a metallic character, i.e., ρ_{zz} decreases with decreasing T .

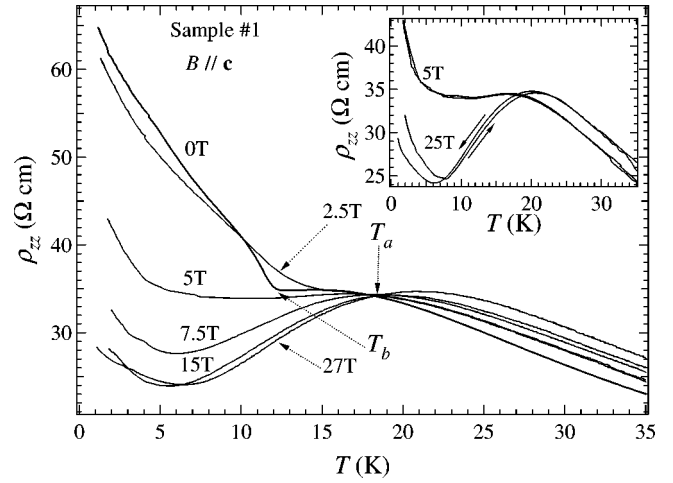


FIG. 3. Interplane resistivity ρ_{zz} as a function of temperature T for several values of magnetic field B , applied along the interplane c axis. For *all* values of B , ρ_{zz} shows a crossover from positive to negative magnetoresistance behavior at a crossover temperature $T_a (> T_b) \approx 18$ K. Inset: ρ_{zz} for both field up and down sweeps (indicated in the figure by arrows) as a function of T and for two values of field 5 and 25 T, respectively. A large hysteresis is observed at 25 T.

(ii) For *all* values of magnetic field, ρ_{zz} shows a crossover from positive to negative magnetoresistance behavior at a crossover temperature $T_a (> T_b) \approx 18$ K.

(iii) The kink observed at T_b is rapidly suppressed by the application of a magnetic field.

The inset of Fig. 3 shows the dependence of ρ_{zz} on temperature T for two values of field $B = 5$ and 25 T, respectively, and for $\theta = 0^\circ$. Arrows indicate increasing and decreasing temperature sweeps. A marked T -dependent hysteresis is observed for $B = 25$ T (as well as smaller, but noticeable hysteresis at 5 T), indicating some sort of first-order domainlike behavior. The observation that all the curves meet at $T_a (> T_b)$ suggests that T_a does not correspond to a thermodynamic phase transition. Instead, it may indicate that charge transport in this system is described by two distinct mechanisms with quite different temperature dependencies and T_a would correspond to the crossover temperature between them. The mechanism that dominates the transport at low temperatures clearly has a strong magnetic field dependence.

Figure 4 displays the magnetoresistance R_{zz} , from sample No. 1, as a function of magnetic field B for $\theta \approx 0^\circ$, and for four different temperatures 1.45, 1.0, 0.7, and 0.50 K, respectively. All curves are vertically displaced for clarity with arrows indicating field-up and field-down sweeps. As previously reported,¹⁷ the resistance decreases by a factor $\geq 65\%$, followed again, by a significant temperature dependent hysteresis. Furthermore, for $T \leq 1$ K and for fields above $B \geq 17$ tesla, Shubnikov-de Haas (SdH) oscillations are observed. This is an indication of the high quality (or long mean free path at high fields) of these τ phase metallic single crystals. The resistivity ratio $\Delta\rho = [\rho(300 \text{ K}) - \rho(4.2 \text{ K})]/\rho(4.2 \text{ K})$ is generally used as a criteria for judging the quality of a metal. Typically, to observe SdH

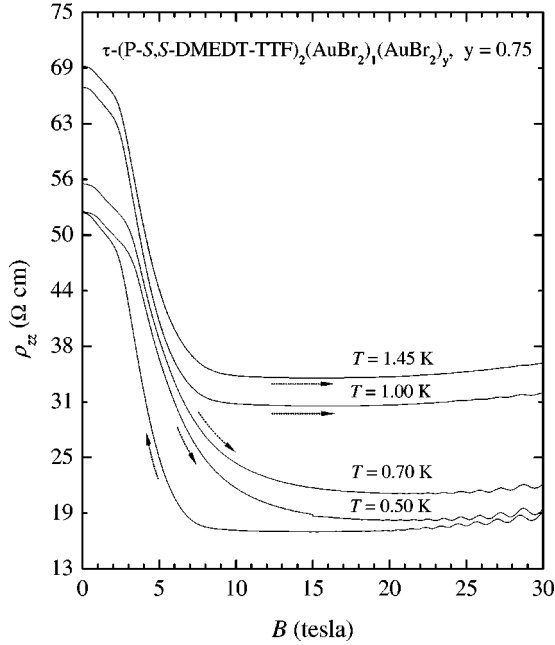


FIG. 4. Interplane resistivity ρ_{zz} (sample No. 1) as a function of B for $\theta=0^\circ$ for several temperatures 1.45, 1.0, 0.7, 0.5 K, respectively. Curves are vertically displaced for clarity. Arrows indicate field-up and field-down sweeps.

oscillations, a $\Delta\rho \sim 100$ or greater is necessary. In the present case, not only is $\Delta\rho$ small, but negative. Here we find $\Delta\rho_{zz} \approx -0.9$ at $B=0$ T and $\Delta\rho_{zz} \approx -0.8$ at $B=27$ T. Hence the mechanism which produces the apparent nonmetallic behavior at lower fields does not compromise the Fermi-liquid properties observed at higher magnetic fields.

The upper panel of Fig. 5 shows the SdH signal as a function of inverse field B^{-1} for $\theta=0^\circ$ and for several values of T , as indicated in the figure. The SdH signal is here defined as $(\sigma - \sigma_b)/\sigma_b$, where σ is the conductance or the inverse of the actual resistivity of our sample (valid if the Hall component is small, which is the case here), and σ_b is the background conductance, obtained by inverting the background resistance. σ_b is obtained by fitting the actual sample resistance to a low-order (4 or less) polynomial. The SdH signal amplitudes, thus defined, may then be directly treated with the standard Lifshitz-Kosevich (LK) formalism⁷ to obtain the effective masses of the carriers in terms of the free electron mass, as well as the Dingle temperature, which describes the impurity level in the material. A fast Fourier transform method (FFT) was used to obtain the SdH amplitudes vs temperature. In the FFT spectrum, shown in the inset of Fig. 5 for $T=0.5$ K, we obtain two peaks at $F_l = 186$ and $F_h = 516$ T, respectively. The lower frequency at F_l can be seen (by eye) as a slight variation of the wave-form amplitudes in the more dominant F_h signal (upper panel, Fig. 5). To further verify that the FFT spectrum was not producing the F_l frequency as an artifact, we independently fit the total SdH signal with the LK expression⁷ for F_h , and then subtracted the fit from the SdH signal. The result is shown in the lower panel of Fig. 5, which clearly shows the presence of the F_l component, as well as its temperature dependence.

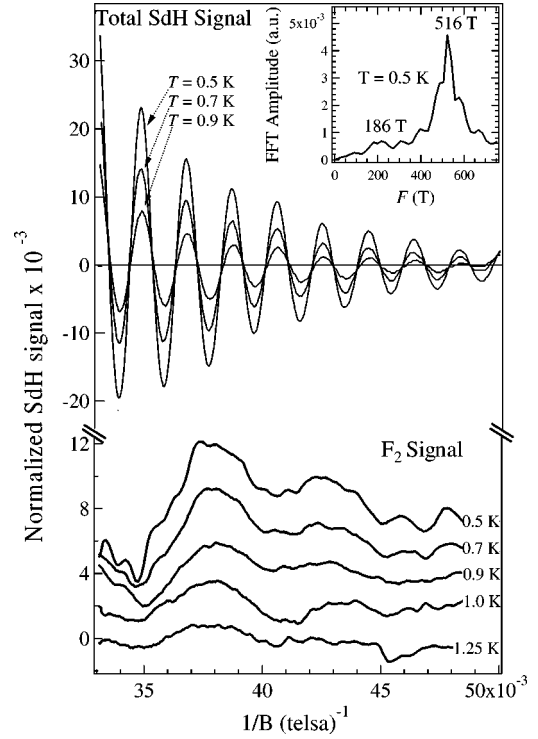


FIG. 5. The SdH signal for τ -[P-(S,S)-DMEDT-TTF]₂(AuBr₂)_y. Upper panel: Total SdH signal as a function of inverse field B^{-1} for $\theta=0^\circ$ for different temperatures T . Inset: The FFT spectrum for the $T=0.5$ K SdH signal. Two frequencies, F_l and F_h appear in the data. Lower panel: The low frequency SdH signal (F_l) obtained by subtraction of the high frequency (F_h) component. (See text for definitions and discussion.)

The observation of two frequencies, i.e., two Fermi surface extreme cross-sectional areas, is surprising since, according to band structure calculations,¹⁸ the FS of this compound is composed of a single and closed star-shaped sheet [see Fig. 1(b)]. Furthermore, from published crystallographic data,¹⁸ the area of the first Brillouin (FBZ) zone is given by $A_{\text{FBZ}} = 72.986 \text{ nm}^{-2}$. Using the Onsager relation $F = A/(h/4\pi^2 e)$, where F is the SdH frequency, A the respective FS cross sectional area, e the electron charge, and h Planck's constant, we obtained 2.4 and 6.8% of the A_{FBZ} for F_l and F_h , respectively. In contrast, the ratio of the area of the calculated closed Fermi surface in Fig. 1(b) to A_{FBZ} is estimated to be 1:8, corresponding to a frequency $F_{\text{FS}} = 955.8$ T. Therefore, the estimated F_{FS} is considerably higher than either value determined in the present work. It is interesting to mention that the fraction of “disordered” anions y , which determines the area of the FS has been found to be time dependent in a related compound τ -[EDO-(S,S)-DMEDT-TTF]₂(I₃)_{1+y}.¹⁹ If in our sample, the anion content y differs from ~ 0.75 , the actual geometry of the FS would necessarily differ from that shown in Fig. 1(b). But this effect would not explain this discrepancy since the area of the FS increases as y decreases for intermediate y . Alternatively, it is possible that the “kink” observed at T_b is the onset of an eventual AF transition; as AF transitions would open partial gaps at the Fermi level and also affect the original geometry of the FS. However, to date no indications

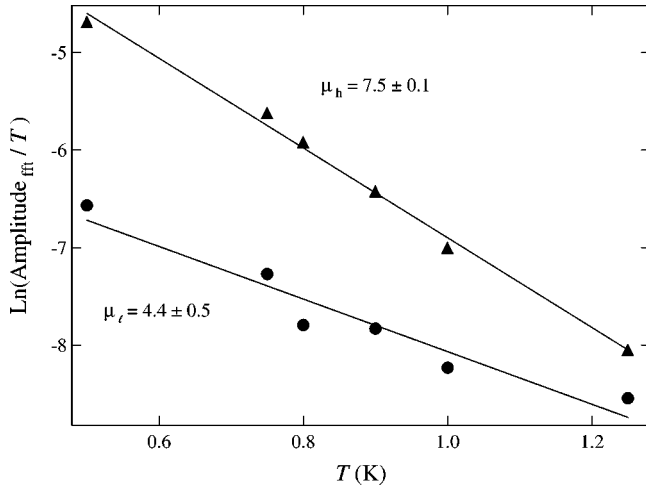


FIG. 6. The logarithm of the FFT amplitudes divided by T , of the SdH signals (from Fig. 5) vs temperature T : F_l (solid squares); F_h (open circles). Solid lines are fits to the Lifshitz-Kosevich formalism, where the slopes provide the effective masses $\mu_l = 4.4 \pm 0.5$ for F_l and $\mu_h = 7.5 \pm 0.1$ for F_h , respectively.

of a phase transition at T_b have been found either in specific heat or in magnetic susceptibility measurements.^{16,18}

Figure 6 shows the logarithm of the SdH amplitudes (from the FFT of the data in Fig. 5) divided by T vs T . The solid lines are a fit to the LK expression $X/\sinh X$ where $X = \alpha \mu_c T/B$, $\alpha = 14.69$ T/K and μ_c is the effective cyclotron mass in relative units of the free electron mass m_e . The slope yields the effective cyclotron masses $\mu_l = 4.4 \pm 0.5$ and $\mu_h = 7.5 \pm 0.1$ for F_l and F_h , respectively. These effective masses are relatively high masses for an organic metal, and in fact these values are not surprising, since the curvature of the proposed star-shaped FS presents singularities at its vertices. Another possible origin for the high mass values is magnetism, given the hysteretic nature of the transport observed. The exchange interaction between carriers and localized moments are known to considerably modify the transport of carriers,²⁵ especially near a metal-insulator transition. In general, complex magnetoresistive behavior (combinations of positive and negative magnetoresistivities as, for example, in manganites) has led to theories for the formation of magnetic polarons,²⁶ i.e., ferromagnetic regions of local moments aligned with the spin of the carrier, via the exchange interaction. However, direct evidence for magnetism in the present case is yet to be observed.

Additional information can be obtained by the Lifshitz-Kosevich formalism⁷ by plotting the amplitude of the SdH oscillations, normalized with respect to $B^{1/2}$. From this, we obtain the Dingle damping factor $R_D = \exp(-\alpha \mu_c T_D/B)$ where $T_D = h/(4\pi^2 k_B \tau)$ (k_B is the Boltzmann constant, μ_c is the carriers effective mass in electronic mass units, and τ is the relaxation time). We obtain $T_D = 1.32 \pm 0.15$ K, which is a small value typical of organic metals,⁷ and indicates the high quality of this τ phase single crystal despite the negative value of $\Delta\rho_{zz}$. Hence the reason SdH oscillations are difficult to see above 1 K is due to the large effective masses, which enhance the LK damping factors.

Figure 7 displays the interplane magnetoresistance R_{zz} as

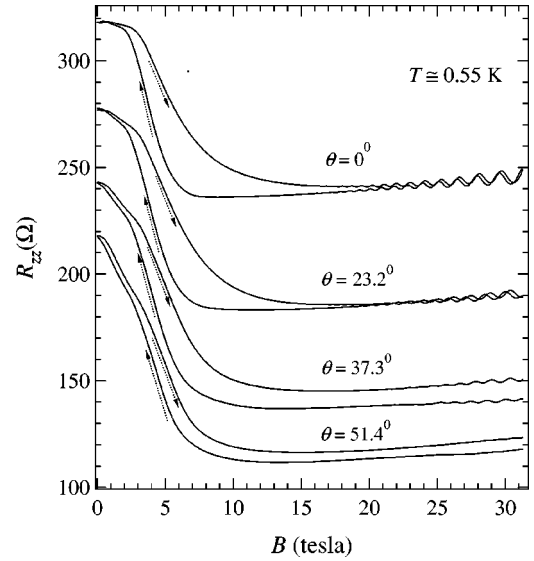


FIG. 7. Interplane magnetoresistance R_{zz} as a function of B at $T \approx 0.55$ K and for several values of the angle θ between B and the interplane c axis. Dotted arrows indicate field up and down sweeps.

a function of magnetic field B at $T \approx 0.55$ K for different values of the angle θ (between B and the interplane c axis), as indicated in the figure. Dotted arrows indicate field up and down sweeps. We find that the hysteresis in the magnetoresistance decreases for increasing angle. The angular dependence of the SdH oscillation frequencies is shown in Fig. 8 for F_l and F_h . The solid lines are fits to the expression $F(\theta) = F(\theta = 0^\circ)/\cos \theta$. The fit provides values of 184 ± 3 and 520 ± 6 tesla for F_l and F_h , respectively. It also clearly indicates that the FS of the τ -[P-(S,S)-DMEDT-TTF]₂(AuBr₂)_y ($y \sim 0.75$) compound is two-dimensional as expected for an anisotropic layered compound.

Figure 9 displays R_{zz} as a function of θ for two values of the in-plane angle $\phi = 0^\circ$ (dotted line) and $\phi = 45^\circ$ (solid line) at $T = 4.2$ K and $B = 14$ T. $\phi = 0$ is defined as the rotation axis normal to the sample edge; consequently, $\phi = 45^\circ$ corresponds to a rotation along one of the diagonals of the square-shaped sample. (A more detailed angular study is described elsewhere.²⁷) Here we find no sign of angular de-

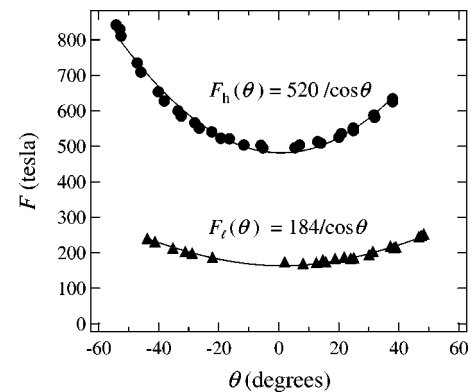


FIG. 8. Angular dependence of both F_l and F_h . Solid lines are fits to the expression $F(\theta) = F(\theta = 0^\circ)/\cos \theta$.

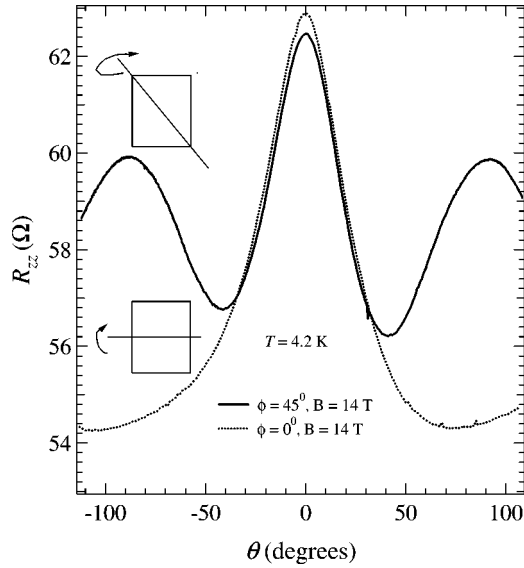


FIG. 9. R_{zz} as a function of θ for two values of the in-plane angle $\phi = 0^\circ$ (solid line) and $\phi = 45^\circ$ (dotted line) at $T = 4.2$ K and $B = 14$ T.

pendent magnetoresistance oscillations (AMRO), which are periodic in $\tan(\theta)$, associated with a warped cylindrical FS topology.^{28,7} Furthermore, the observation of a central peak in R_{zz} , i.e., for $B \parallel I \parallel c$, is quite surprising, since magnetoresistance is not expected under these conditions, as expected from quasiclassical transport theory.

The in-plane resistivity ρ_{xx} as a function of B from sample No. 2 for several different temperatures is presented in Fig. 10(a). The respective temperatures are indicated in the figure. The general behavior of ρ_{xx} is essentially similar to what is observed in ρ_{zz} under field: A large resistivity drop

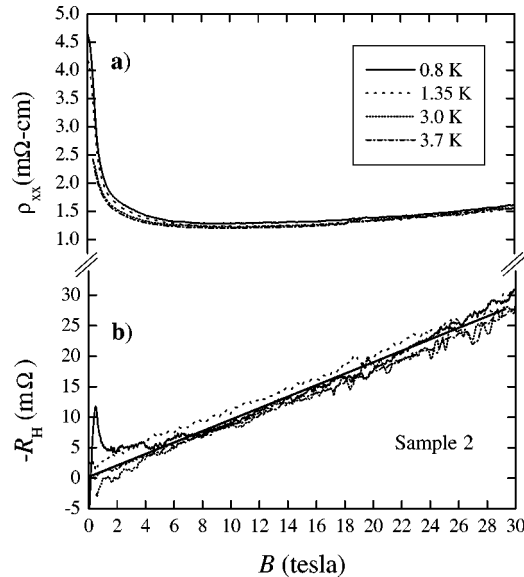


FIG. 10. (a) The in-plane resistivity ρ_{xx} as a function of B from sample No. 2 and for four different temperatures. (b) The Hall resistance R_H as a function of B for the same four values of T as in (a). The solid line is a guide to the eye.

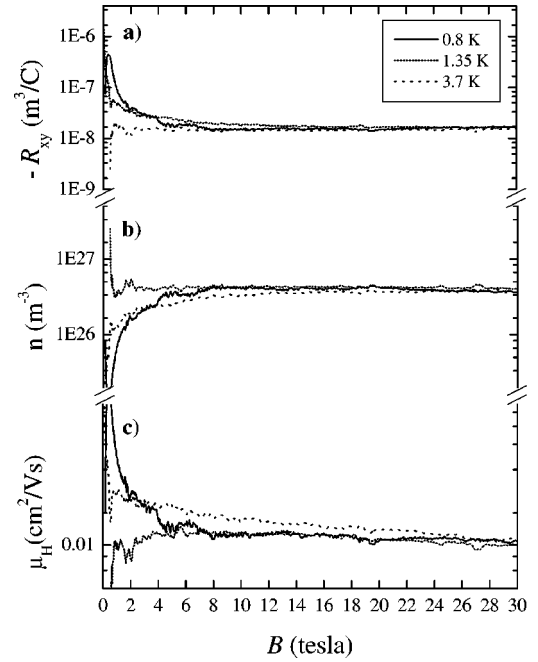


FIG. 11. (a) The Hall constant R_{xy} (see text) as a function of B calculated from the traces shown in Fig. 10(b). (b) The density of carriers n as a function of B obtained from the traces in (a). (c) The Hall mobility $\mu_H \approx R_{xy}/\rho_{xx}$ as a function of field B .

is observed for $B \leq 2$ T (compared with $B \leq 6$ T for ρ_{zz} with sample No. 1). For this sample no quantum oscillations were observed, although sample No. 2 was from the same electrocrystallization cell as sample No. 1. This indicates a variation in quality and/or physical properties may occur during the synthesis process.²⁹ (We note, however, that typically, in organic conductors, ρ_{zz} gives a larger SdH signal than ρ_{xx} .) Figure 10(b) shows the Hall resistance R_H as a function of B and several different temperatures T from Fig. 10(a). R_H is obtained by antisymmetrization of the Hall voltage V_H : $R_H \equiv [V_H(+B) - V_H(-B)]/2I_x$ where $I_x = 50 \mu\text{A}$. We note that R_H is linear in field, as expected for a metal characterized by only one type of carrier, whose sign indicates that electrons are the charge carriers, in agreement with previous results.³⁰ Moreover, R_H is temperature independent below 4.2 K (solid line in this figure is a guide to the eye). The Hall constant $R_{xy} = E_y/j_x \equiv (R_H t/B)$, where E_y is the transverse electric field and j_x is the in-plane density of current, is shown as a function of B in Fig. 11(a), from the traces in Fig. 10(b). Except at low fields, where the Hall signal is too small for an accurate determination, R_{xy} is essentially constant in magnetic field for B up to 30 T. In other words, there is no clear evidence which could indicate that B introduces carriers into the system, hence decreasing its resistivity. An estimation of the density of carriers in our system is provided by the standard expression for the Hall coefficient in a isotropic system: $n = (R_{xy}e)^{-1}$, where e is the electron charge. n is presented in Fig. 11(b) and is basically constant for $B > 4$ T saturating to a value $n \approx 3.75 \times 10^{26} \text{ m}^{-3}$. By multiplying n by the unit cell volume $v = 3676.9 \text{ \AA}^3$ we obtain a value of ≈ 1.4 carriers per unit

cell. This value is remarkably close to the number of acceptor anions $1 + (y \approx 0.75) = 1.75 v^{-1}$, considering the usual uncertainty associated with the sample and contacts geometrical factors as well as the inadequacy of the above expression for describing a temperature dependent Hall effect in an anisotropic 2D system. Consequently, and at least at low temperatures, the number of carriers seems to be given by the number of acceptor anions in this τ phase system. Finally, as $R_{xy} \ll \rho_{xx}$, the Hall mobility, which is proportional to τ_s , the inverse of the scattering rate, is approximately given by $\mu_H \approx R_{xy}/\rho_{xx}$ and is plotted in Fig. 11(c). As seen, μ_H is rather small, on the order of 10^{-2} , and slightly decreases with increasing B , indicating that τ_s increases at higher fields. In the important low field region, where the resistance decreases considerably, it is not possible to directly extract the real behavior of μ_H due to the uncertainties in R_{xy} , as mentioned above. Nevertheless, as R_H is remarkably linear in field, we expect R_{xy} to be essentially constant in the whole field range. As the resistivity decreases by a factor of ~ 3 , μ_H necessarily *increases* by the same factor. At the moment, it is not clear which mechanism is responsible for this magnetic-field induced reduction of τ_s^{-1} .

III. DISCUSSION

The primary findings of the present study are (a) The presence of SdH oscillations clearly indicates the existence of a well defined, two-dimensional Fermi surface. (b) The presence of two SdH frequencies is at odds with the single frequency expected from band structure calculations. (c) The Hall effect shows that the carrier concentration associated with the 2D Fermi surface is independent of magnetic field, even in light of the very large negative magnetoresistance which is observed. (d) The nature of the AMRO data show that the interplane transport may either be incoherent, and/or that the interplane bandwidth is vanishingly small, i.e., the 2D Fermi surface is not warped.

Notably, what remains unknown is an accurate description of the ground state of this unique system. Although, to date magnetic susceptibility measurements do not show evidence for magnetic transitions, there are still arguments that suggest that magnetic order of some kind may play a role. Hysteretic effects in the large, negative magnetoresistance (as well as history-dependent behavior for the in-plane angular dependent magnetoresistance) are suggestive of ferromagnetic order. Since none of the constitutive elements in τ -[P-(S,S)-DMEDT-TTF]₂(AuBr₂) (AuBr₂)_y ($y \sim 0.75$) are magnetic, magnetism can only arise from the electronic bands, or perhaps from localized spins (disorder). Recently, Arita *et al.*³¹ have considered the problem in terms of the relatively flat (low dispersion) bands of the material at the Fermi level. This can give rise to electronic correlations, thereby allowing ferromagnetic spin fluctuations, and consequently an enhanced spin susceptibility. As noted above, however, this enhancement has not yet been observed, nor has any significant ‘‘Curie tail’’ appeared at low temperatures, in magnetic susceptibility measurements.

Another route to understanding the ground state is to consider nesting of the Fermi surface. This is an appealing op-

tion since nesting can lead to a spin or charge density wave (SDW or CDW) ground state, which involves Fermi surface reconstruction, and magnetism in the case of the SDW. Such ground states are known to exhibit hysteretic behavior in magnetic fields, and the reconstructed Fermi surface can exhibit SdH oscillations that differ from those predicted from the band structure calculations. Nevertheless, the observation of two SdH frequencies, which indicates a Fermi surface topology significantly different from Fig. 1, remains a fact. Actually, for a high symmetry FS, as the FS depicted in Fig. 1(b), we expect to find several nesting vectors satisfying a relatively poor nesting condition. This would imply FS reconstruction which would explain the discrepancy between the calculated FS and the FS cross sectional areas detected in this study. However, this hypothesis still requires experimental verification.

In light of the anomalous behavior of the temperature and magnetic field dependent resistivity, the complex structure of the tau-phase compound must be carefully considered. The unit cell along the c axis involves four [P-(S,S)-DMEDT-TTF]₂(AuBr₂) layers, where additionally, there may be some variation in the interlayer ($y \sim 0.75$) composition. This unusually large unit cell configuration may give to the tau phase electronic structure additional degrees of freedom at which we may include the possibility of disorder. In the present case, they may contribute to the very unusual ground state observed in this τ phase organic conductor and simple tests for ferromagnetic, SDW, or CDW behavior may, for instance, not be straightforward.

IV. SUMMARY

In summary we have presented an electrical transport study in the two-dimensional organic conductor τ -[P-(S,S)-DMEDT-TTF]₂(AuBr₂) (AuBr₂)_y (where $y \sim 0.75$) at low temperatures and high magnetic fields B . Both the in-plane and the interplane resistivities show a pronounced negative and hysteretic magnetoresistance, which in some samples is followed by the observation of Shubnikov–de Haas oscillations. Two fundamental frequencies F_l and F_h were detected in the SdH signal, corresponding, respectively, to 2.4 and 6.8% of the area of the first Brillouin zone (A_{FBZ}), which differs significantly from band structure calculations. High effective masses $\mu_l = 4.4 \pm 0.5$ and $\mu_h = 7.5 \pm 0.1$ were obtained for F_l and F_h , respectively. The angular dependence of F_l and F_h reveals the two-dimensional character of the FS, while the absence of frequency beats indicates the absence of warping along the k_z direction. Furthermore, the angle dependent magnetoresistance (AMRO) suggests a FS which is strictly 2D, i.e., the interplane hopping t_c is negligible and/or incoherent. While the Hall constant R_{xy} is field independent, the Hall mobility μ_H increases by a factor of ~ 3 , under moderate magnetic fields. This indicates that B does not introduce carriers into the system, but does decrease the carrier scattering rate τ_s^{-1} .

Our results indicate that this unique, τ phase organic conductor structure is best described as a system of highly two-dimensional Fermi-liquid layers which are nearly decoupled. The details of the mechanisms which give rise to the unusual

low temperature properties remain unresolved, including the identification of the ground state. Although magnetism might be involved, its detection in susceptibility measurements remains elusive. Alternatively, we may speculate that the complex architecture and composition of the unit cell may give rise to additional degrees of freedom which allow the many anomalies and unusual ground state to arise. In this respect, structural, optical, and magnetic resonant studies are needed to further explore this very unique ground state that the tau phase system presents.

ACKNOWLEDGMENTS

We are indebted to V. Dobrosavljevic and K. Murata for helpful discussions and S. MacCall for his help with the SQUID measurements. We also acknowledge support from NSF-DMR 95-10427 and 99-71474 (J.S.B.). One of us (L.B.) is grateful to the NHMFL for sabbatical leave support. The NHMFL was supported through a cooperative agreement between the State of Florida and the NSF through Grant No. NSF-DMR-95-27035.

- ¹T. Ishiguro, K. Yamaji, and G. Saito, in *Organic Superconductors* (Springer-Verlag, Berlin, 1998).
- ²H. Elstrunz, J. Wosnitza, S. Wanka, J. Hagel, D. Schweitzer, and W. Strunz, *Phys. Rev. Lett.* **84**, 6098 (2000); Stéphane Belin, Kamran Behnia, and André Deluzet, *ibid.* **81**, 4728 (1998); I.J. Lee, M.J. Naughton, G.M. Danner, and P.M. Chaikin, *ibid.* **78**, 3555 (1997); H. Mayaffre, P. Wzietek, D. Jérôme, C. Lenoir, and P. Batail, *ibid.* **75**, 4122 (1995); S.M. De Soto, C.P. Slichter, A.M. Kini, H.H. Wang, U. Geiser, and J.M. Williams, *Phys. Rev. B* **52**, 10 364 (1995).
- ³For a recent publication see, for example, T. Nishigushi, M. Kageshima, N. Ara-Kato, and A. Kawazu, *Phys. Rev. Lett.* **81**, 3187 (1998).
- ⁴See for example, L. Degiorgi, M. Dressel, A. Schwartz, B. Alavi, and G. Grüner, *Phys. Rev. Lett.* **76**, 3838 (1996); B.J. Klemme, S.E. Brown, P. Wzietek, G. Kriza, P. Batail, D. Jérôme, and J.M. Fabre, *ibid.* **75**, 2408 (1995); E. Barthel, G. Kriza, G. Quirion, P. Wzietek, D. Jérôme, J.B. Christensen, M. Jorgensen, and K. Bechgaard, *ibid.* **71**, 2825 (1993); S. Tomić, J.R. Cooper, D. Jérôme, and K. Bechgaard, *ibid.* **62**, 462 (1989).
- ⁵J.R. Cooper, W. Kang, P. Auban, G. Montambaux, D. Jérôme, and K. Bechgaard, *Phys. Rev. Lett.* **63**, 1984 (1989); S.T. Hannahs, J.S. Brooks, W. Kang, L.Y. Chiang, and P.M. Chaikin, *ibid.* **63**, 1988 (1989); L. Balicas, G. Kriza, and F.I.B. Williams, *ibid.* **75**, 2000 (1995).
- ⁶See, for example, D.S. Chow, F. Zamborszky, B. Alavi, D.J. Tantillo, A. Baur, C.A. Merlic, and S.E. Brown, *Phys. Rev. Lett.* **85**, 1698 (2000); D.S. Chow, P. Wzietek, D. Fogliatti, B. Alavi, D.J. Tantillo, C.A. Merlic, and S.E. Brown, *ibid.* **81**, 3984 (1998); S.E. Brown, W.G. Clark, F. Zamborszky, B.J. Klemme, G. Kriza, B. Alavi, C. Merlic, P. Kuhns, and W. Moulton, *ibid.* **80**, 5429 (1998).
- ⁷J. Wosnitza, *Fermi Surfaces of Low-Dimensional Organic Metals and Superconductors* (Springer-Verlag, Berlin, 1996).
- ⁸F. Zwick, S. Brown, G. Margaritondo, C. Merlic, M. Onellion, J. Voit, and M. Grioni, *Phys. Rev. Lett.* **79**, 3982 (1997).
- ⁹V. Vescoli, L. Degiorgi, W. Henderson, G. Grner, K.P. Starkey, and L.K. Montgomery, *Science* **281**, 1181 (1998).
- ¹⁰See, for example, E.I. Chashechkina, and P.M. Chaikin, *Phys. Rev. Lett.* **80**, 2181 (1998); G.M. Danner and P.M. Chaikin, *ibid.* **75**, 4690 (1995).
- ¹¹S.P. Strong, D.G. Clarke, and P.W. Anderson, *Phys. Rev. Lett.* **73**, 1007 (1994); D.G. Clarke, S.P. Strong, and P.W. Anderson, *ibid.* **72**, 3218 (1994).
- ¹²A. Sato, E. Ojima, H. Akutsu, H. Kobayashi, A. Kobayashi, and P. Cassoux, *Chem. Lett.* **1998**, 673 (1998).
- ¹³N. Hanasaki, H. Tajima, M. Matsuda, T. Naito, and T. Inabe, *Phys. Rev. B* **62**, 5839 (2000).
- ¹⁴L. Brossard, R. Clerac, C. Coulon, M. Tokumoto, T. Ziman, D.K. Petrov, V.N. Laukhin, M.J. Naughton, A. Audouard, F. Goze, A. Kobayashi, and P. Cassoux, *Eur. Phys. J. B* **1**, 439 (1998).
- ¹⁵G.C. Papavassiliou, Keizo Murata, J.P. Ulmet, A. Terzis, G.A. Mousdis, Harukazu Yoshino, Akihiro Oda, D. Vignolles, and C.P. Raptopoulou, *Synth. Met.* **103**, 1921 (1999); G.C. Papavassiliou, D.J. Lagouvardos, J.S. Zambounis, A. Terzis, C.P. Raptopoulou, K. Murata, N. Shirakawa, L. Ducasse, and P. Delhaes, *Mol. Cryst. Liq. Cryst.* **285**, 83 (1996); A. Terzis (private communication).
- ¹⁶K. Murata, H. Yoshino, Y. Tsubaki, and G.C. Papavassiliou, *Synth. Met.* **94**, 69 (1998).
- ¹⁷H. Yoshino, T. Sasaki, K. Iimura, A. Oda, and G.C. Papavassiliou, *Synth. Met.* **103**, 2010 (1999).
- ¹⁸J.S. Zambounis, G.C. Papavassiliou, D.J. Lagouvardos, A. Terzis, C.P. Raptopoulou, P. Delhaes, L. Ducasse, N.A. Fortune, and K. Murata, *Solid State Commun.* **95**, 211 (1995).
- ¹⁹Keizo Murata, H. Yoshino, Y. Tsubaki, G.C. Papavassiliou, A. Terzis, and J.S. Zambounis, *Synth. Met.* **86**, 2021 (1997).
- ²⁰A. Terzis, B. Hilti, C.W. Mayer, J.S. Zambounis, D.J. Lagouvardos, V.C. Kakoussis, G.A. Mousdis, and G.C. Papavassiliou, *Synth. Met.* **42**, 1715 (1991); G. C. Papavassiliou, V. C. Kakoussis, G. A. Mousdis, A. Terzis, A. Hountas, B. Hilti, C. W. Mayer, J. S. Zambounis, J. Pfeiffer, and P. Delhaes, in *Organic Superconductivity* (Plenum Press, New York, 1990).
- ²¹J. Merino and R.H. McKenzie, *Phys. Rev. B* **61**, 7996 (2000).
- ²²G.C. Papavassiliou, D.J. Lagouvardos, A. Terzis, C.P. Raptopoulou, B. Hilti, W. Hofherr, J.S. Zambounis, G. Rihs, J. Pfeiffer, P. Delhaes, K. Murata, N.A. Fortune, and N. Shirakawa, *Synth. Met.* **70**, 787 (1995).
- ²³G.C. Papavassiliou, Keizo Murata, J.P. Ulmet, A. Terzis, G.A. Mousdis, Harukazu Yoshino, Akihiro Oda, D. Vignolles, and C.P. Raptopoulou, *Synth. Met.* **103**, 1921 (1999); G.C. Papavassiliou, D.J. Lagouvardos, I. Koutselas, K. Murata, A. Graja, J.S. Zambounis, L. Ducasse, J.P. Ulmet, and I. Olejniczak, *ibid.* **86**, 2043 (1997).
- ²⁴A. A. Abrikosov, L. P. Gor'kov, and I. E. Dzyaloshinskii, in *Methods of Quantum Theory in Statistical Physics* (Dover, New York, 1975).
- ²⁵F. Hellman, M.Q. Tran, A.E. Gebala, E.M. Wilcox, and R.C. Dynes, *Phys. Rev. Lett.* **77**, 4652 (1996), and references therein.

- ²⁶See, for example, T. Kasuya and A. Yanase, *Rev. Mod. Phys.* **40**, 684 (1968).
- ²⁷J.S. Brooks, L. Balicas, K. Storr, B.H. Ward, S. Uji, T. Terashima, C. Terakura, J.A. Schlueter, R.W. Winter, J. Mohtasham, G.L. Gard, G.C. Papavassiliou, and M. Tokumoto, cond-mat/0012291 (unpublished); and *Mol. Cryst. Liq. Cryst.* (to be published).
- ²⁸K. Yamaji, *J. Phys. Soc. Jpn.* **58**, 1520 (1989).
- ²⁹G. C. Papavassiliou, V. C. Kakoussis, G. A. Mousdis, A. Terzis, A. Hountas, B. Hilti, C. W. Mayer, J. S. Zambounis, J. Pfeiffer, and P. Delhaes, in *Organic Superconductivity* (Plenum Press, New York, 1990).
- ³⁰N. Fortune, K. Murata, G. C. Papavassiliou, D. J. Lagouvardos, and J. S. Zambounis, in *Electrical, Optical, and Magnetic Properties of Organic Solid State Materials*, edited by A. F. Garito, A. K-Y. Jen, C. Y-C. Lee, L. R. Dalton, MRS Symposia Proceedings No. 328 (Materials Research Society, Pittsburgh, 1994), p. 307.
- ³¹R. Arita, K. Kuroki, and H. Aoki, *Phys. Rev. B* **61**, 3207 (2000).